Published in final edited form as:
J Dent Res. 2008 January ; 87(1): 45–50.

Phenotypic Analysis of *Dlx5* Overexpression in Post-natal Bone

J. Zhang[1,2,†], **J. Zhu**[1,†], **P. Valverde**[1], **L. Li**[1], **S. Pageau**[1], **Q. Tu**[1], **R. Nishimura**[3], **T. Yoneda**[3], **P. Yang**[2], **W. Zheng**[4], **W. Ma**[5], and **J. Chen**[1,*]

[1]Division of Oral Biology, Department of General Dentistry, Tufts University School of Dental Medicine, One Kneeland Street, Boston, MA 02111, USA

[2]College of Stomatology, Shandong University, Shandong Province, China

[3]Department of Biochemistry, Osaka University Graduate School of Dentistry, Osaka, Japan

[4]South Genomics Research Center, Guangzhou, 510800, China

[5]Institute of Genetic Engineering, South Medical University, Guangzhou, 510515, China

Abstract

Dlx5 plays an important role in the embryonic development of mineralized tissues. We hypothesized that *Dlx5* also functions in regulating post-natal bone formation in mice. To prove this hypothesis, we infected 5-day-old bone sialoprotein (BSP)/avian retroviral receptor gene (TVA) transgenic mice with replication-competent retroviral vectors expressing wild-type *Dlx5* (RCAS-*Dlx5*WT) and mutated *Dlx5* at arginine (R) 31 of its homeodomain (RCAS-*Dlx5*RH). Immunohistochemistry indicated that RCAS-*Dlx5*WT increased BSP and osteopontin (OPN) expression, whereas it decreased that of osteocalcin (OC). RCAS-*Dlx5*RH mediated opposite effects. Semi-quantitative RT-PCR confirmed these results. *Ex vivo* overexpression of RCAS-*Dlx5*WT in BSP/TVA calvarial cells promoted, whereas that of RCAS-*Dlx5*RH inhibited, mineralized nodule formation as compared with that in control cells. Our results suggest that *Dlx5* promotes expression of early markers of osteogenic differentiation and increases mineralization post-natally.

Keywords

Dlx5 (distal-less-related gene); homeodomain; BSP/TVA transgenic mice; extracellular matrix proteins; mineralization

INTRODUCTION

Homeodomains are 60-amino-acid-long DNA-binding domains that play a critical role in the genetic control of development. Homeodomains are extremely conserved during evolution, and they show a conserved structure consisting of 3 helical regions (Gehring *et al.*, 1994). The arginine substitution in helix 2 (R31, located at position 31 of the homeodomain) disrupts 1 of 2 arginines that directly interact with the phosphate backbone of the α-strand of the core DNA motif (Gehring *et al.*, 1994), and point mutation at this position has been reported to be associated with human congenital diseases, with alterations in human mineralized tissues (D'Elia *et al.*, 2001). For example, R31 mutation in *Msx*1 leads to selective tooth agenesis (Vastardis *et al.*, 1996), in *Msx*2 to defective skull ossification (Wilkie *et al.*, 2000), in *LMX*1B to nail patella syndrome (including abnormalities of bone, joints, fingernails, and

*corresponding author, jk.chen@tufts.edu.
†authors contributing equally to this work

kidneys) (McIntosh *et al.*, 1998), and in *PITX*2 to Rieger syndrome (including dental hypoplasia, anomalies of the anterior chamber of the eye, and a protuberant umbilicus) (Semina *et al.*, 1996) (APPENDIX Fig.).

Distal-less related genes (*Dlx*) encode homeodomain-containing proteins that play roles in craniofacial patterning, sensory organ morphogenesis and osteogenesis (Merlo *et al.*, 2000). One of the members of the *Dlx* family, *Dlx*5, is expressed in developing skeletal elements, discrete neuronal tissues, and teeth (Simeone *et al.*, 1994). The expression of *Dlx*5 exhibited a stage-specific pattern, with maximal expression occurring in the final stages of osteoblast differentiation *in vitro*, when the extracellular matrix mineralizes (Ryoo *et al.*, 1997). *Dlx*5 is also expressed at the onset of chondrocyte maturation and may regulate the process by promoting conversion of premature proliferating chondrocytes into hypertrophying chondrocytes (Ferrari and Kosher, 2002). Lack of a functional *Dlx*5 in mice results in developmental malformation, including shorter snout, open fontanelle, shorter Meckel's cartilage, defective skull, cleft palate, and deformed mandible (Acampora *et al.*, 1999).

Since mice lacking *Dlx*5 die soon after birth (Depew *et al.*, 2002), the *in vivo* involvement of *Dlx*5 in regulating osteoblast differentiation and bone formation post-natally requires the use of alternative experimental strategies, such as the BSP/TVA model described in our study. In this system, a 4.9-kb murine bone sialoprotein (BSP) promoter is linked to an avian retroviral receptor gene (TVA), and only cells that normally express BSP will express TVA in the BSP/TVA model, and hence will be targeted for viral infection with replication-competent retroviral vectors (RCAS) (Li *et al.*, 2005). BSP is a major non-collagenous protein in mineralized tissues and is expressed in mineralizing tissues (Fisher *et al.*, 1990; Chen *et al.*, 1992; Paz *et al.*, 2005). In the current study, we analyzed the involvement of *Dlx*5 in regulating matrix protein expression and mineralization post-natally by infecting BSP/TVA mice with RCAS vectors expressing the wild-type sequence of *Dlx*5 (RCAS-*Dlx*5WT) or a homeodomain-mutated form of *Dlx*5 (RCAS-*Dlx*5RH). The mutated form of *Dlx*5 (RCAS-*Dlx*5RH) contained a point mutation of R into H at position 166 (R31 of the homeodomain). We chose this residue for mutagenesis based on the evidence mentioned above that, in several transcription factors whose homeodomain is closely related to that of *Dlx*5, such as *Msx1*, *Msx2*, *LMX1B*, and *PITX2*, mutation of this R31 has been associated with alterations in human mineralized tissues. In this study, it was hypothesized that *Dlx*5 also functions in regulating post-natal bone formation.

MATERIALS & METHODS

BSP/TVA Transgenic Mouse Line

The establishment of the BSP/TVA homozygous transgenic line has been described previously (Li *et al.*, 2005). Mice were maintained and used in accordance with recommendations in the *Guide for the Care and Use of Laboratory Animals*, prepared by the Institute on Laboratory Animal Resources, National Research Council, and by guidelines established by the Institutional Animal Care and Use Committee of the Tufts-New England Medical Center in Boston, MA.

Viral Vector Construction

We used an avian retroviral receptor (TVA)-based RCAS retroviral system (Federspiel and Hughes, 1997; Holland and Varmus, 1998). The RCAS empty vector and RCAS-GFP construct were kindly provided by Dr. Stephen Hughes (NCI-Frederick, MD, USA). Intact *Dlx*5 cDNA was kindly provided by Dr. Stephen E. Harris (University of Texas, Health Sciences Center at San Antonio). The PCR product of *Dlx*5 was ligated into Flag-pcDNA3 expression vector at

A supplemental appendix to this article is published electronically only at http://jdr.iadrjournals.org/cgi/content/full/87/1/45/DC1.

BamHI and XbaI sites. The mutated *Dlx*5 (*Dlx*5RH) was generated by *in vitro* mutagenesis with a GeneTailor Site-Directed Mutagenesis System (Invitrogen, Carlsbad, CA, USA). To generate the RCAS viral constructs, we subcloned the 900-bp Hind III-Xba I fragments of pcDNA3-FLAG-*Dlx*5 or mutated *Dlx*5 into a Cla I site in RCAS, using a CLA 12NCO shuttle vector. The viral constructs containing wild-type *Dlx*5 and its mutated form were named RCAS-*Dlx*5WT and RCAS-*Dlx*5RH, respectively. The RCAS empty vector was used as a negative control. To titer infection efficiency in the *in vitro* experiments, we used RCASGFP as a positive control and monitored green fluorescence in the infected cells by fluorescence microscopy.

Production of High-titer Viral Stocks and Infection of BSP/TVA Transgenic Mice

RCAS constructs were transfected into the established chicken fibroblast cell line DF1 (CL-12203), to produce viral stocks as previously described (Tu *et al.*, 2006). Viral supernatant was concentrated, and the viral pellet was re-suspended to a titer of 10^8 cfu/mL and stored at −80°C before use. Thirty 5-day-old BSP/TVA mice (10 mice in each group) were injected intraperitoneally with 500 μL of RCAS-*Dlx*5WT, RCAS-*Dlx*5RH, or empty vector viral stocks, respectively, as described (Li *et al.*, 2005).

In vitro Transduction of RCAS-*Dlx*5WT and RCAS-*Dlx*5RH into BSP/TVA Calvarial Cells

An osteoblast cell line from BSP/TVA mice was established from calvarial bone as previously described (Ecarot-Charrier *et al.*, 1989). Cells were routinely cultured in α-modified essential medium (α-MEM) containing 10% fetal bovine serum and 1% penicillin/streptomycin. Incubation of RCAS-*Dlx*5WT and RCAS-*Dlx*5RH with calvarial cells was performed as previously described (Tu *et al.*, 2006).

RNA Isolation and Reverse-transcriptase Polymerase Chain-reaction (RT-PCR) Analysis

Total RNA was isolated with TRIzol Reagent (GibcoBRL/Life Technologies, Gaithersburg, MD, USA) and was used for RTPCR with SuperScript™ one-step RT-PCR with platinum Taq (Invitrogen). Specific primers for mouse BSP, OPN, ALP, OC, and GAPDH have been described previously (Li *et al.*, 2005). PCR products were photographed and quantified with UVP Image software (UVP, Inc., Upland, CA, USA). GAPDH amplification was performed for normalization purposes.

Western Blot Analysis

Preparation of protein lysates, SDS-PAGE, and Western blot analyses were performed as previously described (Chen *et al.*, 1992; Valverde *et al.*, 2005). Detection of overexpressed *Dlx*5 or mutated *Dlx*5 was carried out with rabbit anti-FLAG polyclonal antibody (anti-FLAG®, 2.5 μg/mL; Sigma, St. Louis, MO, USA) and a horseradish-peroxidase-conjugated goat anti-rabbit IgG antibody (US Biological, Swampscott, MA, USA). Detection of β-actin was used as a loading control. The immunoreactions were detected by chemiluminescence with a BioImaging System (UVP).

Immunohistochemistry

Tissues were processed for immunohistochemistry as described previously (Meinel *et al.*, 2005). Immunohistochemical studies were performed with rabbit polyclonal antibodies against BSP (a gift from Dr. L. Fisher, NIH/NIDCR), OPN (a gift from Dr. L. Fisher, NIH/NIDCR), and OC (from US Biological, Swampscott, MA, USA) at dilutions of 1:200 – 1:300. A non-specific IgG was used as negative control. Slides were assessed and photographed by light microscopy (Carl Zeiss, Inc., Oberkochen, Germany). The localization and intensity of immunohistochemical staining in bone tissues were studied by modified semi-quantitative methods, as previously described (Chen *et al.*, 1991; Paz *et al.*, 2005). In brief, on each slide

there were tissue sections from all 3 groups. The relative intensities of immunohistochemical staining were classified as intense (+++), moderate (++), weak (+), or negative (−). For each slide, the intensity of staining in the control group was classified as moderate, and staining intensity and tissue sections from the other 2 groups were compared with this standard. Stronger staining than control was classified as intense (+++), lower as weak (+), and no staining as negative. All slides were coded to prevent the introduction of examiner bias.

Mineralization Assays *in vitro*

In vitro alizarin red staining was performed essentially as described (Tu *et al.*, 2006), after calvarial cells were maintained in culture medium supplemented with 5 mM β-glycerophosphate and 50 μg/mL of ascorbic acid for 14 days. Digital images of the stained cultures were taken at 10× magnification. Bone nodule number was counted in 6 different fields of each well and in 3 independent experiments.

Statistical Analysis

Results are expressed as mean ± SE of 3 or more independent experiments. We used one-way ANOVA to test significance, using the software package Statgraphic statistical graphics system (STSC, Inc., Rockville, MD, USA). Values of p lower than 0.05 were considered statistically significant.

RESULTS

BSP/TVA-driven Overexpression of *Dlx*5 and Mutated *Dlx*5

To confirm the tissue specificity of viral targeting, we performed Western blot analysis with an anti-FLAG antibody and/or detection of GFP fluorescence. Infection of BSP/TVA mice with RCAS-*Dlx*5 led to positive anti-FLAG immunoreaction in bone tissues, but not in the liver. To confirm further that the viral targeting would be restricted to cells expressing TVA, we performed *ex vivo* infection studies with RCAS-GFP in calvarial cells. Whereas more than 80% of the calvarial cells from BSP/TVA mice exhibited green fluorescence, calvarial cells from wild-type mice were GFP negative (Fig. 1B). In addition, calvarial cells from BSP/TVA mice that were infected *ex vivo* with RCAS-*Dlx*5WT and RCAS-*Dlx*5RH showed a positive immunoreaction for the FLAG antibody, whereas those from wild-type mice demonstrated a lack of immunoreaction in Western blot analysis (Fig. 1C).

*Dlx*5 Overexpression Alters the Expression Pattern of Extracellular Matrix Proteins

Nine days after infection of BSP/TVA transgenic mice, we performed immunohistochemical analyses to evaluate the bone phenotype and expression of the extracellular matrix proteins BSP, OPN, and OC. Infection with RCAS-*Dlx*5WT resulted in an increase in BSP and OPN expression levels, and a decrease in those of OC in calvarial and mandibular tissues, as compared with levels in control animals. In contrast, infection with RCAS-*Dlx*5RH led to a decrease in BSP and OPN and an increase in OC expression levels, as compared with levels in control mice (Fig. 2).

Overexpression of *Dlx*5 and Mutated *Dlx*5 in BSP/TVA Calvarial Cells Determined Different Expression Patterns of Extracellular Matrix Proteins

Calvarial tissues were also subjected to semi-quantitative RTPCR analyses (Fig. 3). Infection with RCAS*Dlx*5WT increased BSP and ALP within the first 3 wks after infection, as compared with control cells. In addition, it increased OPN and decreased OC expression levels from the 2nd to the 4th wks after infection. Infection with RCAS-*Dlx*5RH resulted in the significant up-regulation of OC expression levels from the 2nd to the 4th wks after infection. RCAS-*Dlx*5RH

also decreased the expressions of BSP, OPN, and alkaline phosphatase (ALP) at some of the time-points at which the RCAS-*Dlx*5WT effects were significant.

Calvarial Cells Overexpressing Mutated *Dlx*5 Exhibited a Slower Mineralization Rate Than Did Those Overxepressing Wild-type *Dlx*5

BSP/TVA calvarial cells infected with RCAS-*Dlx*5WT became consistently mineralized 2 and 3 wks after infection, and even 1 wk after infection in some experiments (Figs. 4A, 4B). Cells infected with RCAS-*Dlx*5RH exhibited a lower number of bone nodules at all times examined than did cells infected with RCAS-*Dlx*5WT or control vectors (Figs. 4A, 4B).

DISCUSSION

In this study, we analyzed the involvement of *Dlx*5 in the post-natal expression of osteoblast differentiation markers and in mineralization. Immunohistochemical and RT-PCR analyses indicated that *Dlx*5 increased BSP, OPN, and ALP expression levels, whereas it decreased those of OC. Increases in the expression of ALP and BSP occurred during wks 1–3, while changes in the expression of OPN and OC were seen in wks 2–4. ALP and BSP are both early markers of osteogenic differentiation, while OPN and OCN are mid- and late markers of osteoblasts, respectively, which might be the reason why changes in expression levels of ALP and BSP appeared earlier than those of OCN and OPN (Chen *et al.*, 1992; Lekic *et al*., 1996; Volk *et al.*, 2005; Abe *et al.*, 2006). The effects of mutated *Dlx*5 were opposite to those obtained with wild-type *Dlx*5. Overexpression of *Dlx*5 in ROS 17/2.8 osteoblast-like cells was previously found to decrease OC promoter activity and endogenous OC mRNA levels, whereas antisense inhibition of *Dlx*5 increased OC gene transcription (Ryoo *et al*., 1997). A different report demonstrated that overexpression of *Dlx*5 in chick calvarial osteoblast cultures (Tadic *et al.*, 2002) also increased ALP, OPN, and BSP mRNA levels, as described in our study. Loss of OC expression in mice leads to a phenotype marked by higher bone mass and bones of improved functional quality (Ducy *et al*., 1996), while ALP activity is required for the mineralization process to occur (Murshed *et al.*, 2005). OPN and BSP play roles in both mineralization and bone resorption (Ganss *et al.*, 1999; Sodek *et al*., 2000; Valverde *et al*., 2005; Wang *et al*., 2006). OPN-deficient mice were reported to exhibit increased mineral content and increased crystal size/perfection consistent with *in vitro* data, indicating that OPN can promote osteoclast recruitment and function and inhibit mineral formation and mineral crystal growth (Sodek *et al*., 2000). Recombinant BSP can also promote both bone formation and bone resorption (Ganss *et al.*, 1999; Valverde *et al.*, 2005; Wang *et al.*, 2006). When one considers that BSP/TVA bones exhibited a different pattern of extracellular matrix protein expression before or after infection with *Dlx*5 or mutated *Dlx*5, but did not exhibit other significant macroscopic differences, it is tempting to speculate that *Dlx*5 may play a role in controlling the functional quality of post-natal bone by decreasing OC expression. The apparent lack of effects of *Dlx*5 in affecting bone mass post-natally might be the result of the opposite effects of OC, BSP, and OPN in regulating bone formation and bone resorption.

Overexpression of *Dlx*5 increased the ability of BSP/TVA calvarial cells to mineralize *in vitro*, whereas overexpression of mutated *Dlx*5 decreased their mineralization potential. Homozygous mice lacking *Dlx*5 gene (Acampora *et al.*, 1999) exhibited defective osteogenesis and an increase in OC expression, pointing to a role for *Dlx*5 in bone formation during embryonic development. Since a point mutation at R31 of the homeodomain of *Dlx*5 was found to inhibit mineralization and increase OC expression in our study, it is likely that the effect of this mutation is due to haploinsufficiency, as has been described for other related homeodomain-containing proteins (D'Elia *et al.*, 2001). This notion is supported by the observation that deletion of an entire homeodomain-containing gene elicits a phenotype that is very similar to that induced by point mutations at the homeodomain. However, since mutated

*Dlx*5 was overexpressed post-natally and only in bone-like cells in our study, the phenotype was found to be milder than in the *Dlx*5 knockout study, but consistent with the role of *Dlx*5 in promoting osteogenesis.

To summarize, we have demonstrated that *Dlx*5 promotes the expression of early markers of osteoblast differentiation during post-natal bone development and induces formation of bone nodules. Future studies combining the use of the BSP/TVA transgenic model and of targeted point mutations in homeodomain - containing proteins are expected to lead to a wealth of information about the involvement of these transcription factors in the post-natal regulation of osteogenesis.

Acknowledgments

This study was supported by NIH grants DE14537 and DE16710 to JC. We appreciate the secretarial assistance of Amanda Fix.

REFERENCES

Abe T, Nomura S, Nakagawa R, Fujimoto M, Kawase I, Naka T. Osteoblast differentiation is impaired in SOCS-1-deficient mice. J Bone Miner Metab 2006;24:283–290. [PubMed: 16816922]

Acampora D, Merlo GR, Paleari L, Zerega B, Postiglione MP, Mantero S, et al. Craniofacial, vestibular and bone defects in mice lacking the Distal-less-related gene Dlx5. Development 1999;126:3795–3809. [PubMed: 10433909]

Chen J, Zhang Q, McCulloch CA, Sodek J. Immunohistochemical localization of bone sialoprotein in foetal porcine bone tissues: comparisons with secreted phosphoprotein 1 (SPP-1, osteopontin) and SPARC (osteonectin). Histochem J 1991;23:281–289. [PubMed: 1938474]

Chen J, Shapiro HS, Sodek J. Development expression of bone sialoprotein mRNA in rat mineralized connective tissues. J Bone Miner Res 1992;7:987–997. [PubMed: 1442213]

D'Elia AV, Tell G, Paron I, Pellizzari L, Lonigro R, Damante G. Missense mutations of human homeoboxes: a review. Hum Mutat 2001;18:361–374. [PubMed: 11668629]

Depew MJ, Lufkin T, Rubenstein JL. Specification of jaw subdivisions by Dlx genes. Science 2002;298:381–385. [PubMed: 12193642]

Ducy P, Desbois C, Boyce B, Pinero G, Story B, Dunstan C, et al. Increased bone formation in osteocalcin-deficient mice. Nature 1996;382:448–452. [PubMed: 8684484]

Ecarot-Charrier B, Bouchard F, Delloye C. Bone sialoprotein II synthesized by cultured osteoblasts contains tyrosine sulfate. J Biol Chem 1989;264:20049–20053. [PubMed: 2584207]

Federspiel MJ, Hughes SH. Retroviral gene delivery. Methods Cell Biol 1997;52:179–214. [PubMed: 9379950]

Ferrari D, Kosher RA. Dlx5 is a positive regulator of chondrocyte differentiation during endochondral ossification. Dev Biol 2002;252:257–270. [PubMed: 12482714]

Fisher LW, McBride OW, Termine JD, Young MF. Human bone sialoprotein. Deduced protein sequence and chromosomal localization. J Biol Chem 1990;265:2347–2351. [PubMed: 2404984]

Ganss B, Kim RH, Sodek J. Bone sialoprotein. Crit Rev Oral Biol Med 1999;10:79–98. [PubMed: 10759428]

Gehring WJ, Affolter M, Burglin T. Homeodomain proteins. Annu Rev Biochem 1994;63:487–526. [PubMed: 7979246]

Holland EC, Varmus HE. Basic fibroblast growth factor induces cell migration and proliferation after glia-specific gene transfer in mice. Proc Natl Acad Sci USA 1998;95:1218–1223. [PubMed: 9448312]

Lekic P, Sodek J, McCulloch CA. Osteopontin and bone sialoprotein expression in regenerating rat periodontal ligament and alveolar bone. Anat Rec 1996;244:50–58. [PubMed: 8838423]

Li L, Zhu J, Tu Q, Yamauchi M, Sodek J, Karsenty G, et al. An *in vivo* model to study osteogenic gene regulation: targeting an avian retroviral receptor (TVA) to bone with the bone sialoprotein (BSP) promoter. J Bone Miner Res 2005;20:1403–1413. [PubMed: 16007338]

McIntosh I, Dreyer SD, Clough MV, Dunston JA, Eyaid W, Roig CM, et al. Mutation analysis of LMX1B gene in nail-patella syndrome patients. Am J Hum Genet 1998;63:1651–1658. [PubMed: 9837817]

Meinel L, Fajardo R, Hofmann S, Langer R, Chen J, Snyder B, et al. Silk implants for the healing of critical size bone defects. Bone 2005;37:688–698. [PubMed: 16140599]

Merlo GR, Zerega B, Paleari L, Trombino S, Mantero S, Levi G. Multiple functions of Dlx genes. Int J Dev Biol 2000;44:619–626. [PubMed: 11061425]

Murshed M, Harmey D, Millan JL, McKee MD, Karsenty G. Unique coexpression in osteoblasts of broadly expressed genes accounts for the spatial restriction of ECM mineralization to bone. Genes Dev 2005;19:1093–1104. [PubMed: 15833911]

Paz J, Wade K, Kiyoshima T, Sodek J, Tang J, Yamauchi M, et al. Tissue- and bone cell-specific expression of bone sialoprotein is directed by a 9.0 kb promoter in transgenic mice. Matrix Biol 2005;24:341–352. [PubMed: 15970437]

Ryoo HM, Hoffmann HM, Beumer T, Frenkel B, Towler DA, Stein GS, et al. Stage-specific expression of Dlx-5 during osteoblast differentiation: involvement in regulation of osteocalcin gene expression. Mol Endocrinol 1997;11:1681–1694. [PubMed: 9328350]

Semina EV, Reiter R, Leysens NJ, Alward WL, Small KW, Datson NA, et al. Cloning and characterization of a novel bicoid-related homeobox transcription factor gene, RIEG, involved in Rieger syndrome. Nat Genet 1996;14:392–399. [PubMed: 8944018]

Simeone A, Acampora D, Pannese M, D'Esposito M, Stornaiuolo A, Gulisano M, et al. Cloning and characterization of two members of the vertebrate Dlx gene family. Proc Natl Acad Sci USA 1994;91:2250–2254. [PubMed: 7907794]

Sodek J, Ganss B, McKee MD. Osteopontin. Crit Rev Oral Biol Med 2000;11:279–303. [PubMed: 11021631]

Tadic T, Dodig M, Erceg I, Marijanovic I, Mina M, Kalajzic Z, et al. Overexpression of Dlx5 in chicken calvarial cells accelerates osteoblastic differentiation. J Bone Miner Res 2002;17:1008–1014. [PubMed: 12054155]

Tu Q, Valverde P, Chen J. Osterix enhances proliferation and osteogenic potential of bone marrow stromal cells. Biochem Biophys Res Commun 2006;341:1257–1265. [PubMed: 16466699]

Valverde P, Tu Q, Chen J. BSP and RANKL induce osteoclastogenesis and bone resorption synergistically. J Bone Miner Res 2005;20:1669–1679. [PubMed: 16059638]

Vastardis H, Karimbux N, Guthua SW, Seidman JG, Seidman CE. A human MSX1 homeodomain missense mutation causes selective tooth agenesis. Nat Genet 1996;13:417–421. [PubMed: 8696335]

Volk SW, Diefenderfer DL, Christopher SA, Haskins ME, Leboy PS. Effects of osteogenic inducers on cultures of canine mesenchymal stem cells. Am J Vet Res 2005;66:1729–1737. [PubMed: 16273904]

Wang J, Zhou HY, Salih E, Xu L, Wunderlich L, Gu X, et al. Site-specific *in vivo* calcification and osteogenesis stimulated by bone sialoprotein. Calcif Tissue Int 2006;79:179–189. [PubMed: 16969594]

Wilkie AO, Tang Z, Elanko N, Walsh S, Twigg SR, Hurst JA, et al. Functional haploinsufficiency of the human homeobox gene MSX2 causes defects in skull ossification. Nat Genet 2000;24:387–390. [PubMed: 10742103]

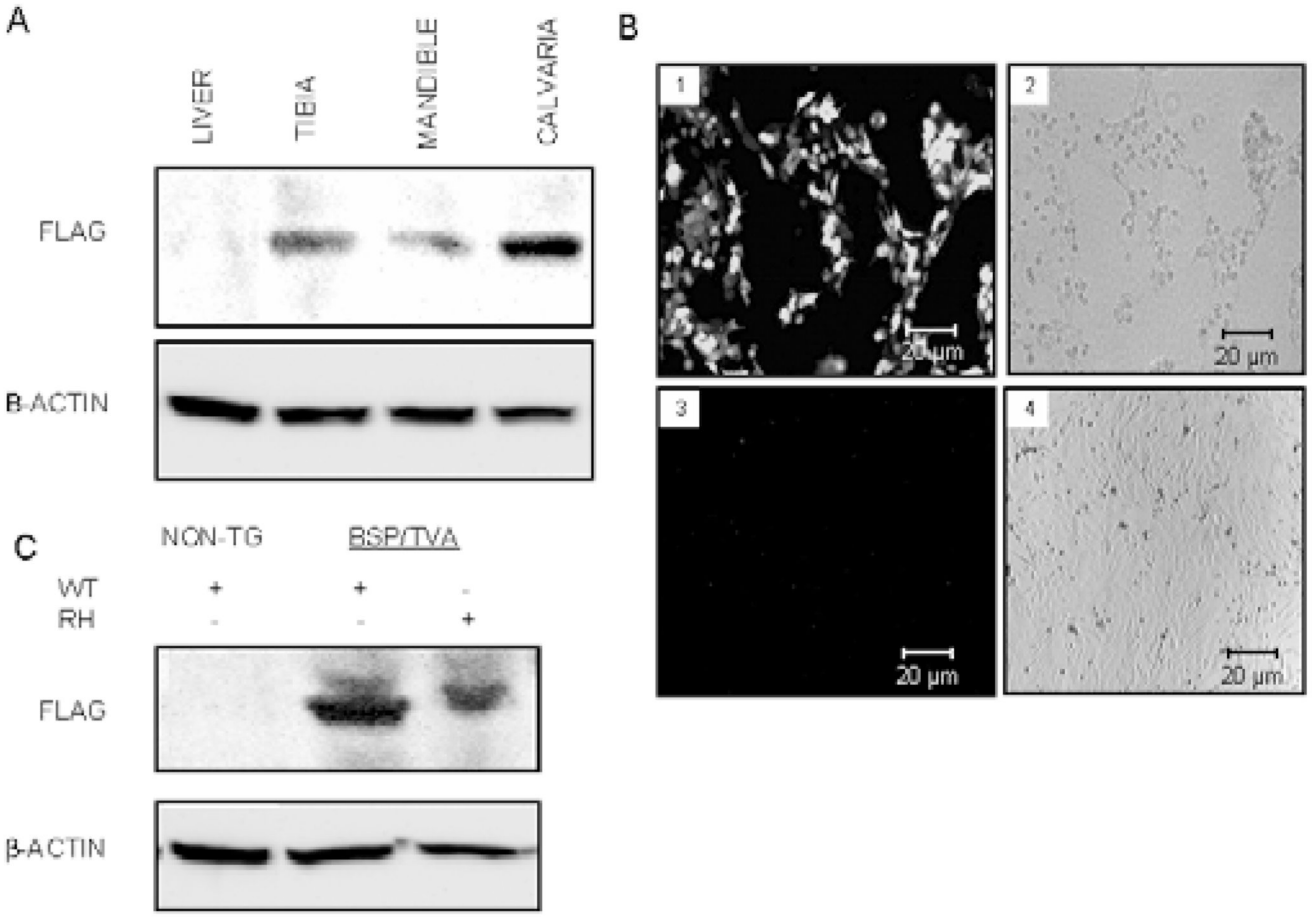

Figure 1.

BSP/TVA-driven *Dlx5* or mutated *Dlx5* overexpression in mineralized tissues and calvarial cultures. Western blot analyses were performed with tissues from BSP/TVA mice 4 days after infection with RCAS-*Dlx*5 (i.e., on day 9) and calvarial cells 3 days after *in vitro* infection with RCAS-*Dlx*5 or RCAS-*Dlx*5RH. **(A)** Expression analysis upon *in vivo* delivery of *Dlx5* viral constructs. BSP/TVA mice were infected with RCAS-*Dlx5*, and expression of overexpressed *Dlx5* was detected with an anti-FLAG antibody on day 9. An antibody for β-actin was used as a loading control. Protein lysates were obtained from tibial, mandibular, and calvarial tissues isolated from BSP/TVA mice infected with the RCAS-*Dlx*5 construct and from a representative soft tissue (*i.e.*, liver). **(B)** GFP expression analyses upon *ex vivo* infection of RCAS-GFP into calvarial cells from BSP/TVA transgenic and non-transgenic mice. Calvarial cells from BSP/TVA mice (1,2) or wild-type mice that did not express TVA (2,4) were transfected with the RCASGFP construct. We used GFP expression to titer infection efficiency and to confirm the specificity of the overexpression to cells that express TVA 3 days after the infection. The *in vitro*-infected cells were photographed by fluorescence (1,3) and phase contrast (2,4) microscopy. Green fluorescence was detected in infected cells from BSP/TVA mice (1), but not in those of normal mice, due to the lack of TVA expression (3). **(C)** Western blot analysis upon *ex vivo* delivery of viral constructs. The analysis was performed with protein lysates from calvarial cells derived from non-transgenic mice (without TVA expression) before and after being infected *ex vivo* with RCAS-*Dlx*5. Calvarial cells from BSP/TVA mice were infected *ex vivo* with RCAS-*Dlx5*WT or RCAS-*Dlx5*RH viral constructs. Expression of exogenous *Dlx5* constructs and the loading control β-actin were detected as described above.

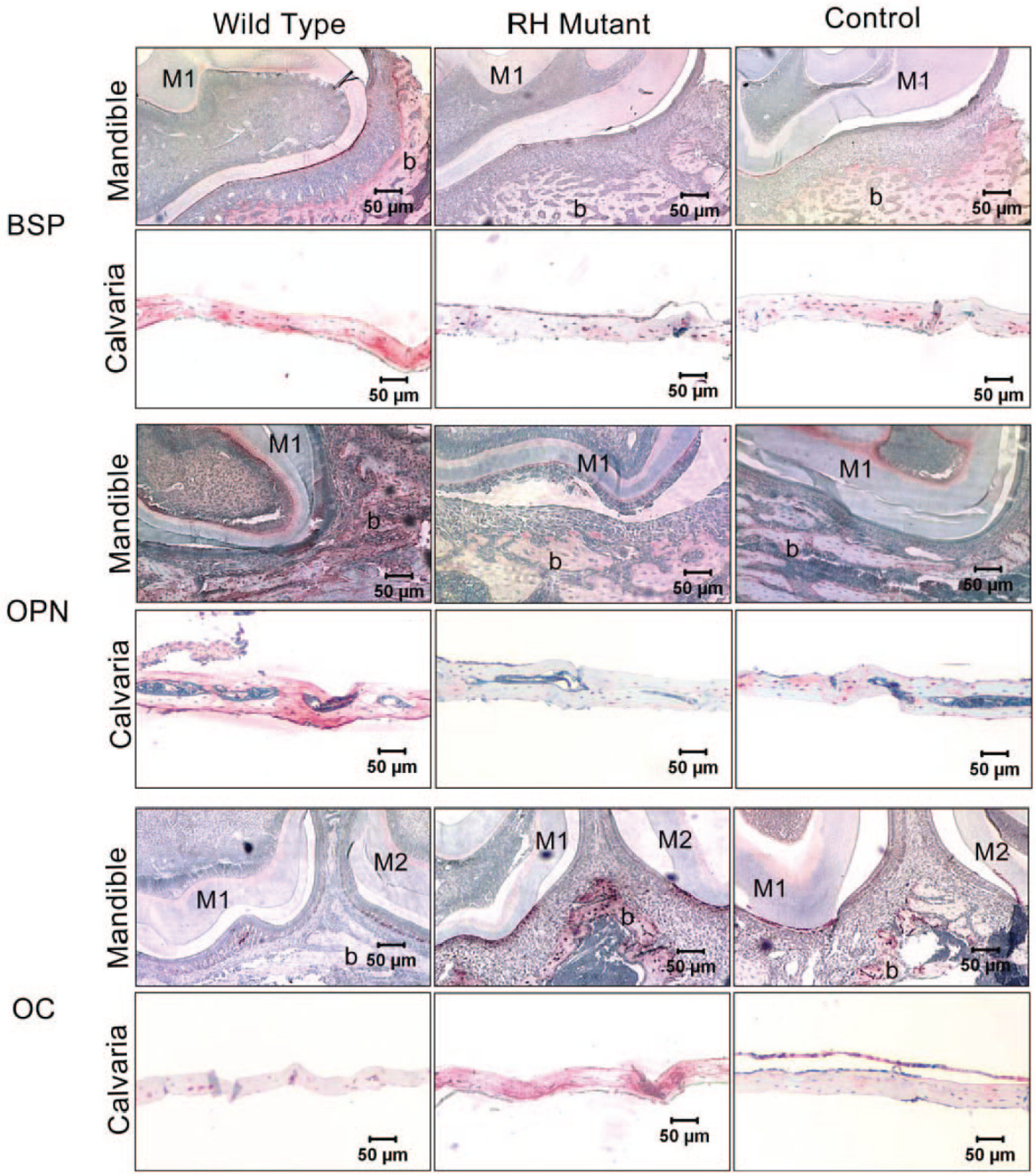

Figure 2.

Immunohistochemical analysis of extracellular matrix proteins OPN, BSP, and OC in bone tissues of BSP/TVA overexpressing mutated *Dlx5* (RH mutant), wild-type *Dlx5* (Wild-type), and empty vector (Control). Nine days after infection of BSP/TVA with viral constructs, bones were isolated, and immunohistochemistry was performed to determine the expression of OPN, BSP, and OC in calvarial and mandibular tissues. Expression levels of OPN, BSP, and OC in mandibles were shown in transverse sections of the developing first and/or second molars and the surrounding tissues at the cementumenamel junction. In control mandibular tissues, BSP and OCN were both moderately expressed in the cells (osteoblasts and osteocytes) and in bone matrix associated with the alveolar bone surface. BSP expression in mandibular tissues isolated

from the wild-type group was up-regulated in the alveolar bone surface area, and moderate expression can be detected in the odontoblast layer. However, BSP expression in mandibular tissues isolated from RH mutant group was down-regulated, and there is no evident BSP expression above background. In contrast, OCN expression in the wild-type group was weaker than that in the RH mutant group. OPN expression in control mandibular tissues can also be detected in the alveolar bone surface (osteoblasts, osteocytes, and bone matrix), as well as the odontoblast layer. OPN expression in the corresponding areas in the wild-type group and the RH mutant group was up-regulated and down-regulated, respectively. Expressions of BSP, OPN, and OCN are all evident in the osteocytes and bone matrix of control calvarial tissues. While BSP and OPN expression levels are increased in the wild-type group and decreased in the RH mutant group, OCN expression level is down-regulated in the wild-type group and up-regulated in the RH mutant group. M1, the first mandibular molar; M2, the second mandibular molar; b, bone.

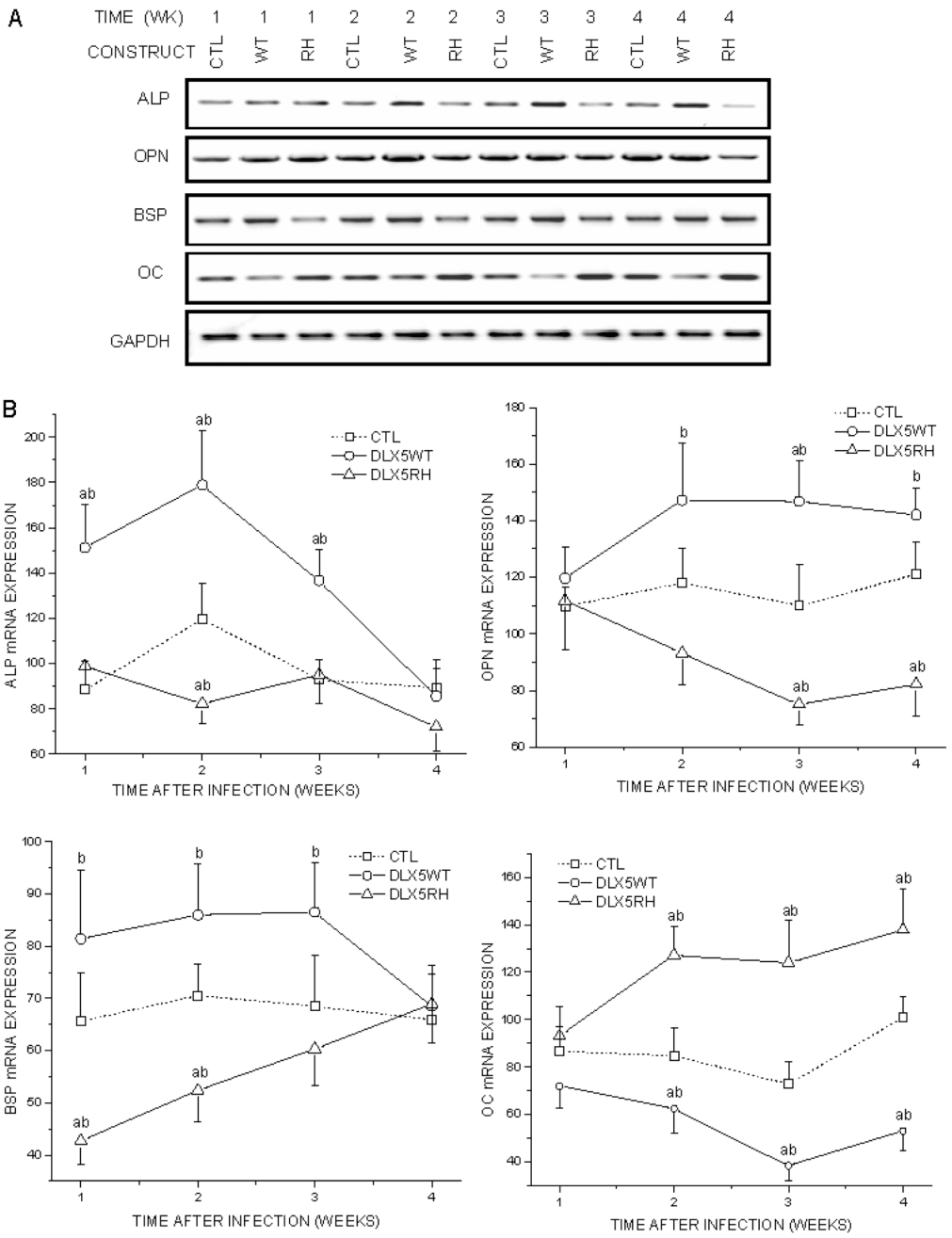

Figure 3.

Semi-quantitative RT-PCR analysis for markers of osteoblast differentiation, including extracellular matrix proteins and ALP. BSP/TVA mice were infected with RCAS-*Dlx5*WT (WT), RCASDlx5RH (RH), or RCAS empty vector as a control (CTL). Calvarial tissues were isolated for 1 to 4 wks after infection, and their expression levels of ALP, OPN, BSP, and OC were analyzed by semi-quantitative RT-PCR. Expression of GAPDH was used as a loading control. **(A)** Representative RT-PCR experiment. **(B)** Normalized mRNA expression of ALP, OPN, BSP, and OC. Results (in arbitrary units) are expressed as the mean ± SE from 3 different experiments. Values of $p < 0.05$ were considered significantly different ($^{a}p < 0.05$ vs. CTL at every specific time point; $^{b}p < 0.05$ WT vs. RH).

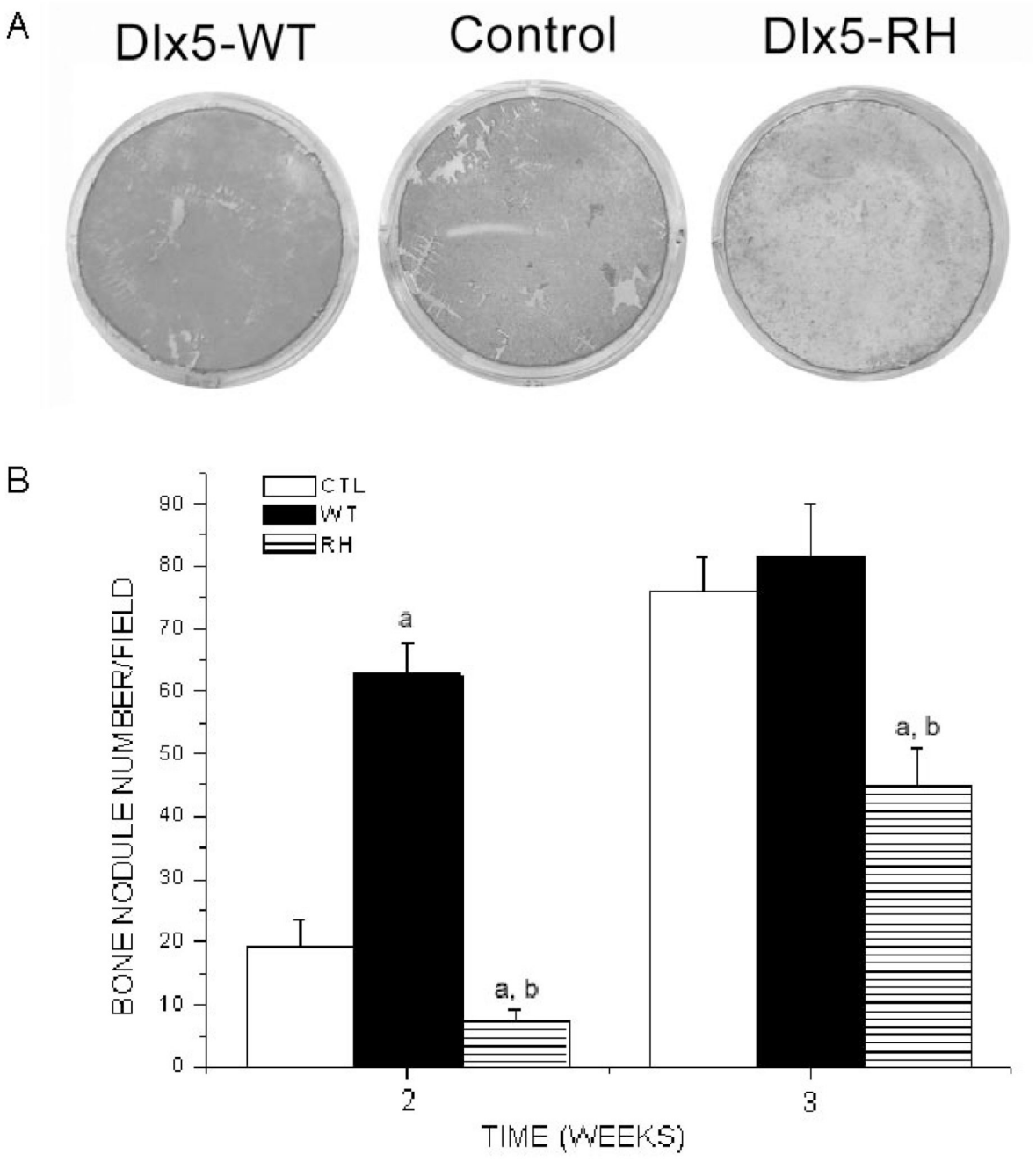

Figure 4.

Effects of RCAS-*Dlx5*WT, RCAS-*Dlx5*RH, or empty RCAS vector in bone nodule formation of calvarial cells expressing TVA. Calvarial cells from BSP/TVA mice were infected with RCAS empty vector (Control), wild-type *Dlx5* (*Dlx5*-WT), and mutated *Dlx5* (*Dlx5*-RH). The formation of *in vitro* mineralization nodules was determined by alizarin red-S histochemical staining, and the number of nodules was counted under a microscope at different time-points (1, 2, and 3 wks). **(A)** Representative example of alizarin red-S staining 2 wks after infection and osteogenic differentiation. **(B)** Numbers of nodules obtained 2 and 3 wks after infection and osteogenic differentiation. Results are the mean ± SE from 3 different experiments. Values

of $p < 0.05$ were considered significantly different ([a]$p < 0.05$ vs. CTL at every time-point; [b]$p < 0.05$ RH vs. WT at every time-point).